



Cite this: DOI: 10.1039/c6dt04409c

Enhancement in catalytic proton reduction by an internal base in a diiron pentacarbonyl complex: its synthesis, characterisation, inter-conversion and electrochemical investigation†

Zhimei Li,^a Zhiyin Xiao,^b Fenfen Xu,^a Xianghua Zeng^b and Xiaoming Liu^{*b}

The reaction of a tripodal ligand (**H₂L**) with a {S₂N} donor-set with tri-iron dodecacarbonyl in toluene leads to the isolation of a diiron pentacarbonyl complex **1** as a model for the sub-site of the [FeFe]-hydrogenase. Protonation of this complex under CO (1 atm.) forms quantitatively the hexacarbonyl complex **2H⁺** with a pendant pyridinium group. Infrared spectroscopic investigations indicate that its pendant pyridinium group dissociates to give hexacarbonyl complex **2** which forms subsequently the pentacarbonyl complex **1**. The electrochemistry of these complexes has been investigated. Complex **2H⁺** exhibits electrocatalysis on proton reduction at a potential more positive by over 200 mV compared to that for other neutral diiron hexacarbonyl complexes. This catalysis is enhanced under a CO atmosphere by freeing the bound base group which acts as a proton relay in the catalysis.

Received 21st November 2016,

Accepted 11th January 2017

DOI: 10.1039/c6dt04409c

www.rsc.org/dalton

1 Introduction

Over nearly 20 years, chemistry related to [FeFe]-hydrogenase, which has a diiron centre as its active sub-site, Fig. 1a,^{1–4} has attracted considerable attention due to its relevance to hydrogen production. The research on mimicking the diiron centre of the [FeFe]-hydrogenase has made significant progress in the view point of understanding the catalytic mechanism of the enzyme and why nature chooses such unique “building blocks” to construct its catalytic machinery.^{5–12} For example, studies on the model complexes with a {Fe₂S₃}-core led to

finally pinning down the oxidation state of the distal iron in the diiron sub-site of the enzyme.¹³ Challenges of this type are often encountered in the studies of many other metallo-enzymes.¹⁴ The first mimics for the H-cluster framework of the [FeFe]-hydrogenase demonstrated that the {Fe₄S₄} cluster as an electron mediator has electronic communication with the diiron centre as evidenced by the CO stretching band shift of the diiron sub-unit.¹⁵ Thorough investigation into the electrochemistry of diiron mimics by a number of groups around the world including our group revealed that the diiron centre may undergo two-electron reduction by exhibiting one single redox peak in the cyclic voltammogram *via* an ECE mechanism.^{16–21} The coupled chemical reaction is an isomerisation that probably is the breaking of one of the four Fe–S bonds, which generates an intermediate whose reduction potential is likely no more negative than that of the first reduction (potential inversion). This observation may have relevance to explain why the diiron active centre of the enzyme operates without an over-potential.

One significant progress was made in the identification of the nature of the middle atom of the dithiolate bridging the two iron atoms in the subunit of the enzyme. It turned out that only the diiron mimics bearing azodithiolate can function after being assembled into the apo-HydA1 protein.²² It is believed that some proximal base groups around the sub-site in the enzyme may have a role to play in proton transfer in catalysis.^{2,23} Indeed, a pendant basic group in an iron-hydride complex may relay protons.²⁴ Recently, there have been reports showing that the protonated internal base in model complexes

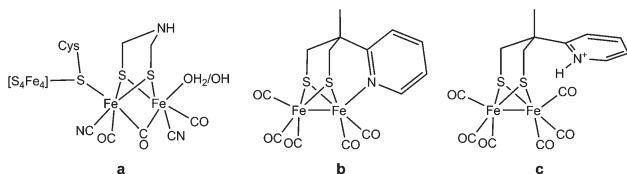


Fig. 1 The diiron units in (a) the H-cluster of the [FeFe]-hydrogenase, (b) the model complex, **1** and (c) the protonated model complex, **2H⁺**.

^aSchool of Chemistry, Nanchang University, Nanchang 330031, China

^bCollege of Biological, Chemical Sciences and Engineering, Jiaxing University, Jiaxing 314001, China. E-mail: xiaoming.liu@mail.zjxu.edu.cn,

xiaoming.liu@ncu.edu.cn; Fax: +86 (0)573 83643937; Tel: +86 (0)573 83643937

† Electronic supplementary information (ESI) available. See DOI: 10.1039/c6dt04409c

could transfer the proton to the Fe–Fe bond forming hydride.^{25–28} Rauchfuss and co-workers first reported the synthesis of a structural model to mimic the proposed aza-bridge head in the diiron sub-unit of the enzyme, in which a base group was introduced *via* a ligand, azadithiolate.²⁹ Although the base group can be protonated, it does not seem to have significant improvement in the catalysis of proton reduction except for the positive shift of the reduction potential.³⁰ This potential shift could be contributed to the effect of positive charge introduced by protonation. Due to the same inspiration, a base group was also introduced into model complexes by simply reacting the diiron hexacarbonyl complex with a free base, for instance, a pyridine derivative.^{31,32}

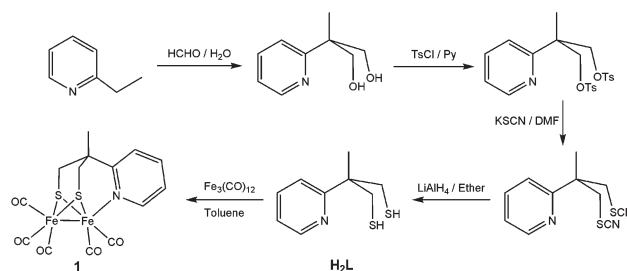
We reported preliminarily model complexes with a {Fe₂S₂N}-core,³³ in which the N-containing functional group is an integrated part of the entire organic moiety of the bridge head. One of the reported model complexes possessed a pyridine group, which gives a hexacarbonyl complex upon protonation, Fig. 1b and c. In this complex (**1**), the hemi-labile Fe–N bond underwent CO-substitution reaction and this CO substitution was facilitated by protonation by following a “square scheme”.³³ Herein, we further report the synthesis, and full characterisation of the pyridine containing model complexes, particularly the electrochemistry, and electrocatalysis of the hexacarbonyl complex (Fig. 1c) towards proton reduction.

2 Results and discussion

2.1 Synthesis of the tripodal ligand (H₂L) and the model complex (**1**)

Ligand **H₂L** was synthesised using a modified literature method.³⁴ In an autoclave, an aqueous solution of formaldehyde (excess) and 2-ethylpyridine was heated for 2–3 days to give a mixture of products, 2-methyl-2-(pyridin-2-yl)ethanol and 2-methyl-2-(pyridin-2-yl)propane-1,3-diol, in equilibrium with their precursor. Distillation for purifying the desired product 2-methyl-2-(pyridin-2-yl)propane-1,3-diol as employed in the literature procedure was not adopted due to the high boiling points of these compounds. Instead, flash chromatography was used to isolate the diol. This approach improved both the yield and efficiency. For the rest of the reactions in the preparations of ligand **H₂L** and its diiron carbonyl complex, **1**, general procedures used for the preparation of model complexes with a {Fe₂S₃}-core were followed.^{13,35} A schematic description of the syntheses is shown in Scheme 1.

Heating a mixture of ligand **H₂L** and Fe₃(CO)₁₂ in toluene at 110 °C gave the desired pentacarbonyl products **1** in the yield of 35% after flash chromatography purification. It should be noticed that, after re-examination of the reaction of dithiol (**H₂L**) with Fe₃(CO)₁₂, another interesting diiron pentacarbonyl complex ([Fe₂{(SCH₂)₂C(CH₃)(2-C₅H₈N)}(CO)₅]) with the pyridinyl ring of the ligand hydrogenated partially should be obtained, as we reported otherwise.³⁶ Single crystals of complex **1** suitable for X-ray diffraction were grown from acetonitrile solution through either slow solvent evaporation or



Scheme 1 Synthetic route of the ligand **H₂L** and its diiron carbonyl complex **1**.

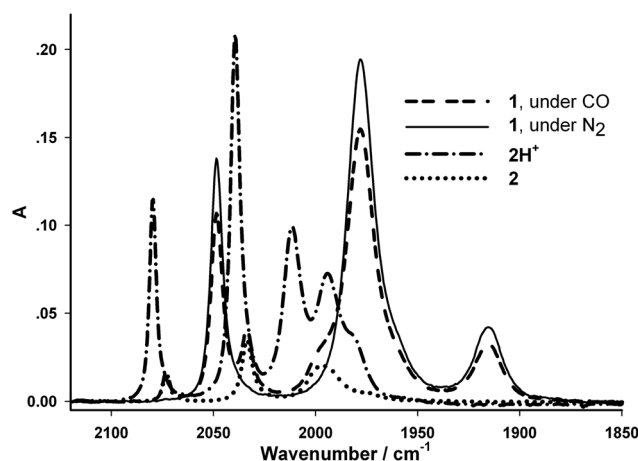


Fig. 2 FTIR spectra of the complexes in dichloromethane: **1** under N₂/CO (1 atm.), **2** and 2H⁺ under N₂.

being stored in a freezer at –25 °C. Complex **1** in dichloromethane shows three major CO stretching bands (Fig. 2) with a characteristic spectral pattern for model complexes of the {Fe₂S₃}-core reported before.^{7,13} But the FTIR absorption bands of complex **1** shift to lower frequencies by a few wavenumbers compared to the SMe containing pentacarbonyl complex,¹³ which shows that the pyridine N atom is a slightly better electron donor than SMe. The electron donating capability of these ligands is in agreement with their basicity. Although there is no pK_a value available for ligand **H₂L**, it would be sensible to refer this ligand to 2-methylpyridine whose pK_a is about 6 in aqueous solution.³⁷ Compared to the pK_a value of thioether, –6.8,³⁸ ligand **H₂L** is a much stronger base than SMe.

2.2 Structural analysis

Complex **1** and its protonated hexacarbonyl 2H⁺ were crystallographically characterized and preliminarily reported, Fig. 3.³³ The crystal data and experimental details are summarized in Table S1.† Selected bonds and bond angles of some of the complexes were tabulated for comparison in Table 1, in which the Fe1 is designated to the Fe atom proximal to the pyridine/pyridinium ring. Compared to other complexes containing the

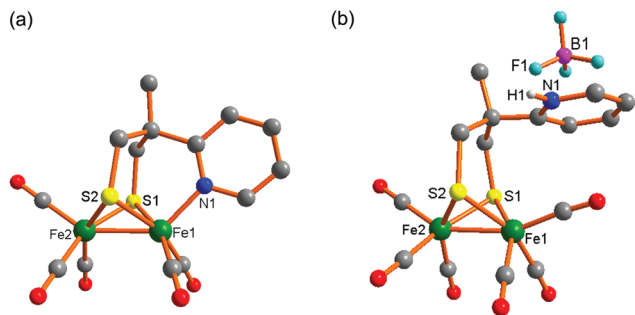


Fig. 3 Crystallographic structures of complexes **1** (a) and **2H⁺** (b).

Table 1 Selected bond lengths (Å) and angles (°) for complexes **1** and **2H⁺**

Bond length/angle	1	2H⁺
Fe1–Fe2	2.5325(3)	2.4990(4)
Fe1–S1	2.2538(5)	2.2814(5)
Fe2–S1	2.2602(5)	2.2595(5)
Fe1–S2	2.2461(5)	2.2509(6)
Fe2–S2	2.2572(5)	2.2573(5)
Fe1–N	2.0099(14)	
Fe1–S1–Fe2	68.255(14)	66.778(15)
Fe1–S2–Fe2	68.438(14)	67.330(15)
S1–Fe1–N	93.10(4)	
S2–Fe1–N	93.96(4)	

{Fe₂S₃}-core,^{13,35,39} the Fe1–Fe2 bond length (2.5325(3) Å) in complex **1** is slightly longer. This bond lengthening is attributed to the π -interaction between the metals and the pyridine group. The π -back bonding interaction between the Fe1 atom and the pyridine ring strengthens the Fe1–N bonding. When the π -back bonding interaction does not exist in complex **2H⁺**, the Fe1–Fe2 bond length is 2.4990(4) Å, comparable to the bond lengths of this type found in most diiron hexacarbonyl complexes.^{40–42}

This π -back bonding interaction is also evidenced by the UV/vis spectrum of complex **1**, Fig. S6.† An absorption band for complex **1** shows a red-shift down to 376 nm compared to 370 nm for other pentacarbonyl complexes.³⁹ This red-shift renders the complex dark green colour instead of the normally observed dark brown for other pentacarbonyl complexes.¹³ This π -back bonding interaction is further demonstrated by the improvement in the reversibility of the reduction of complex **1** (*vide infra*).

For both pentacarbonyl,^{13,35,39} including complex **1**, and hexacarbonyl complexes,^{40–42} the four Fe–S bonds which bridge the two iron atoms are nearly identical in bond length with a standard deviation less than 0.007 Å. But for complex **2H⁺**, the Fe1–S2 bond length at the same side as the title pyridinium group is at least 0.02 Å longer than the other three (Table 1). This bond lengthening is probably due to the steric effect caused by the pyridinium group. Compared to the orientation of the bound pyridine in complex **1**, the pyridinium group in complex **2H⁺** turns nearly by 90°.

2.3 Protonation of complex **1**

Under a CO (1 atm.) atmosphere, addition of HBF₄·Et₂O to a solution of complex **1** in organic solvent yielded quantitatively the hexacarbonyl complex **2H⁺** with a pendant pyridinium group, Fig. 1c. However, under a N₂ atmosphere, adding one equivalent of HBF₄·Et₂O to complex **1** formed a mixture of complex **1** and complex **2H⁺**, Fig. S7.† Increasing one more equivalent acid led to the disappearance of complex **1** and formation of complex **2H⁺**. No other carbonyl complex was observed as illustrated by their IR spectra of the protonation reactions. The addition of an excess base (triethylamine) could fully deprotonate complex **2H⁺** to complex **1** with a recovery of about 70%. At a low temperature (<10 °C), the addition of one equivalent of acid HBF₄·Et₂O to the solution of complex **1** in dichloromethane generates a mixture of the bridging hydride complex **1H⁺** and the hexacarbonyl complex **2H⁺**, Fig. 4. The spectrum of the bridging hydride **1H⁺** is similar to that of the amine containing complex ([Fe₂(μ -H){(SCH₂)₂C(CH₃)(2-CH₂NH₂)}(CO)₅]⁺, Table S2†) reported previously but with less stability.³³ This bridging hydride decays to hexacarbonyl complex **2H⁺** by “cannibalising” CO when raising the temperature.

It has been known that metal hydrides undergo intramolecular transfer.⁴³ This intramolecular hydride transfer strongly depends on the basicity of the hydride and its acceptor. Metal hydride is commonly regarded as a base in Brønsted/Lowry acid–base theory.⁴⁴ However, acidic metal hydrides are observed and a typical example of this kind is the classic iron carbonyl hydride, H₂Fe(CO)₄ with pK_a = 4.4.⁴⁵ Indeed, the bridging hydride **1H⁺** reacts with Et₃N to restore its parent complex **1**, which shows its acidity. In the conversion of the bridging hydride **1H⁺** to **2H⁺**, the hydride may undergo intramolecular transfer. As we reported before, the transfer may adopt two pathways as suggested by DFT calculations.³⁶ In either pathway, the bridging hydride in the species **1H⁺** switches to the terminal hydride first and this terminal hydride eventually transfers to the nearby base. One of the

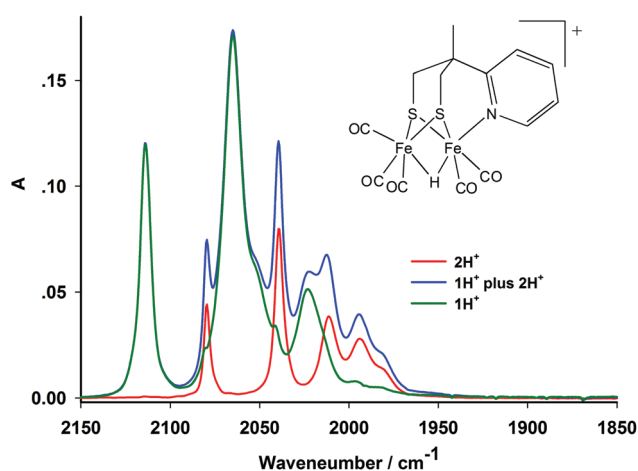
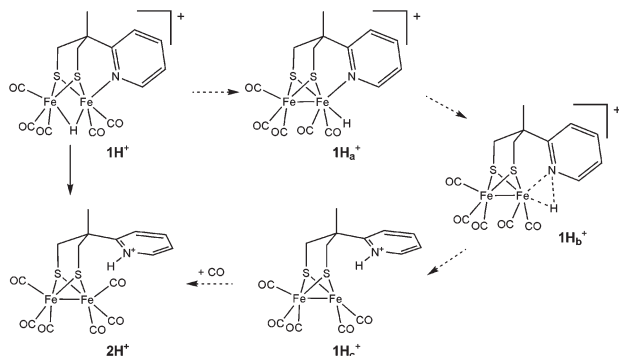


Fig. 4 Infrared spectrum of complex **1** in dichloromethane at low temperature after the addition of one equivalent of the acid, HBF₄·Et₂O, which comprises the contributions from both **1H⁺** (inset) and **2H⁺**.



Scheme 2 Proposed pathway for the conversion of 1H^+ to 2H^+ .

possible pathways is shown in Scheme 2.³⁶ In the end, the pyridine group is protonated and cleaved as pyridinium salt. Consequently, a vacant site is exposed at the proximal $\{\text{Fe}(\text{CO})_2\}$ unit for CO binding.

In an absolutely dry solvent, the spectrum of complex 2H^+ shows a characteristic spectral pattern for the hexacarbonyl diiron complex. However, any trace amount of water in a solvent in which its solution is prepared will significantly alter its infrared spectrum, Fig. 5 (black). The multiple bands between 2100 and 1900 cm^{-1} indicate multiple species in the solution of hexacarbonyl 2H^+ . Further examination of this spectrum and de-convolution show that there are spectral features belonging to complexes 2 (green), 1 (blue) and 2H^+ (red), Fig. 5, respectively. The relationship of these species is depicted in Scheme 3. The equilibrium between complexes 1 and 2 was observed when the solution of complex 1 was saturated with CO,³³ Fig. S8.†

2.4 Electrochemistry and electrocatalysis towards proton reduction of complexes 1 and 2H^+

Complex 1 is electrochemically investigated in dichloromethane. As shown in Fig. 6, it has one reduction process at

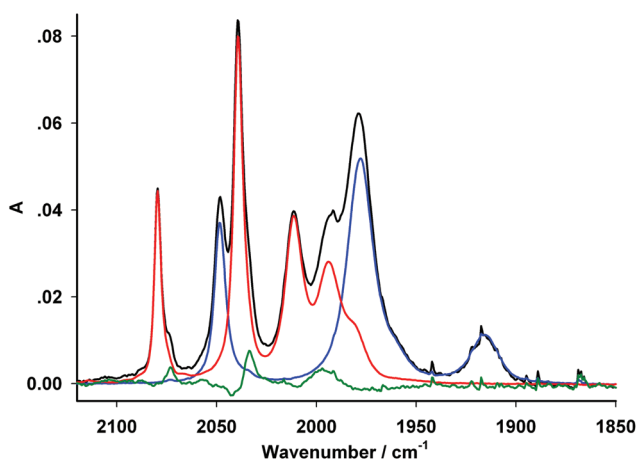
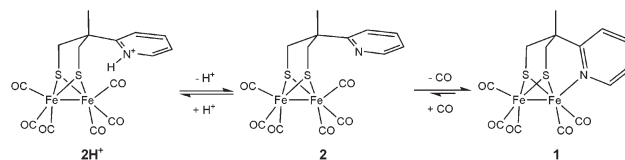


Fig. 5 FTIR spectrum of the solution of complex 2H^+ (black) in "wet" dichloromethane which, in fact, comprises the spectra of complexes 1 (blue), 2H^+ (red) and 2 (green), respectively.



Scheme 3 Equilibrations among complexes established based on the infrared spectrum of complex 2H^+ in dichloromethane.

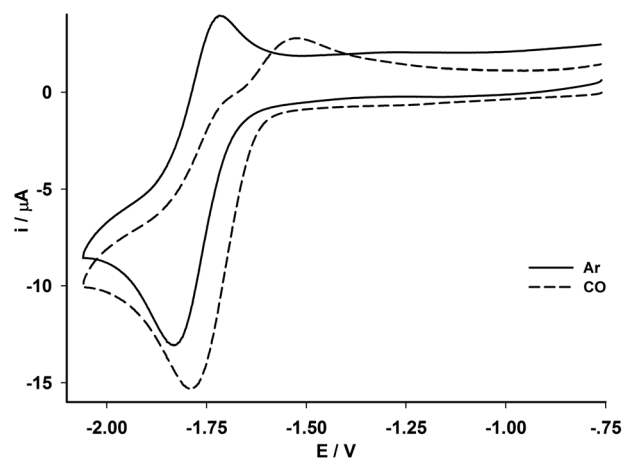


Fig. 6 Cyclic voltammograms of complex 1 (3.7 mmol L^{-1}) under an Ar/CO atmosphere in dichloromethane at the scanning rate of 0.1 V s^{-1} at 298 K.

-1.83 V and one irreversible oxidation process at 0.22 V (Fig. S9†). The reduction process of complex 1 is essentially similar to those complexes containing the $\{\text{Fe}_2\text{S}_3\}$ -core except for enhanced reversibility.¹³ This is attributed to the moderate π -accepting nature of the pyridine group as discussed above. Under a CO atmosphere, the electrochemistry of complex 1 changed dramatically. Its quasi-reversibility under an Ar atmosphere was lost. The reduction potential shifted positively with a slight increase in current intensity. To understand this significant change in electrochemistry, following observations should be bore in mind. Complex 1 undergoes conversion into complex 2 under a CO atmosphere (Scheme 3) and reduction of hexacarbonyl complexes occurs at a potential more positive than that of pentacarbonyl by over 100 mV .⁴⁶ Thus, most likely, the reduction potential shift could be attributed to the formation of complex 2 under a CO atmosphere. This conversion can be facilitated by the reduction of complex 2 whose reduction potential is more positive than that of complex 1. Varying the scanning rate increased steadily the peak current intensity of the returning wave, Fig. S10.† The plot of the reduction peak current against the square-root of the scanning rate shows good linearity ($R = 0.998$), Fig. S10† (inset), suggesting the diffusion-controlled nature of the reduction.

The electrochemistry of complex 2H^+ in dichloromethane is fundamentally different from other neutral hexacarbonyl complexes, for instance $[\text{Fe}_2(\text{pdt})(\text{CO})_6]$ (pdt = propane-1,3-dithiolate).⁴⁶ As shown in Fig. 7, there are two reduction processes,

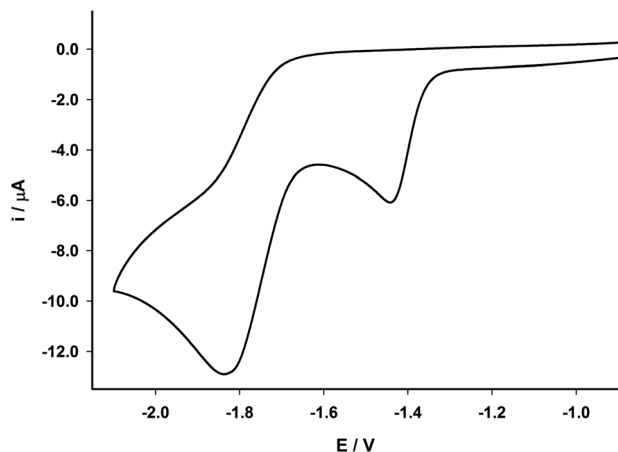


Fig. 7 Cyclic voltammogram of complex 2H^+ (3.4 mmol L^{-1}) under an Ar atmosphere in dichloromethane at the scanning rate of 0.1 V s^{-1} at 298 K.

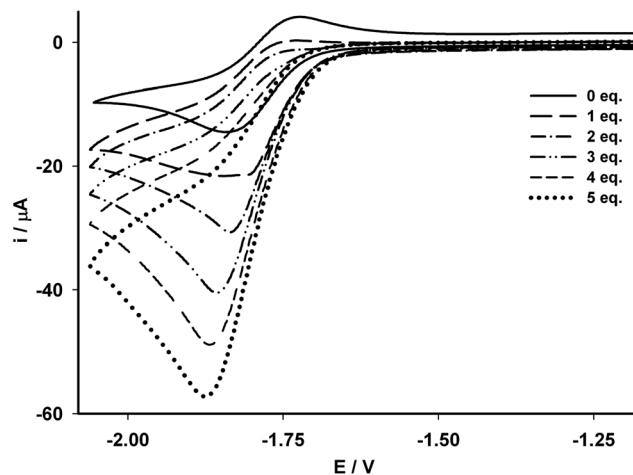


Fig. 8 Cyclic voltammograms of complex **1** (3.96 mmol L^{-1}) with the addition of lutidinium under an Ar atmosphere in dichloromethane at the scanning rate of 0.1 V s^{-1} at 298 K.

one at -1.44 V and the other at -1.84 V . The peak current of the latter process is about 1.6 fold stronger than that of the first one. The peak potential separation between the two processes is about 400 mV . As discussed above, complex 2H^+ dissociates into **2** which forms further complex **1** in the absence of external CO. It is known that protonation of a pendant base of a diiron model complex can bring the reduction to more positive potential by a few hundred mV.^{47,48} Therefore, the first reduction at -1.44 V is assigned to the reduction of complex 2H^+ and the second process to that of complex **1**.

In the oxidation potential range, complex 2H^+ shows a major irreversible peak at 0.86 V and a minor peak at 0.20 V , Fig. S11.† The potential of the small peak is comparable to that of the oxidation process of complex **1**, Fig. S9.† Thus, these oxidations are assigned to complexes 2H^+ and **1**, respectively. This is further experimental evidence showing that the major reduction of complex 2H^+ has the origin of complex **1**.

Upon addition of a weak acid, for example lutidinium, complex **1** shows electrocatalysis on proton reduction and the catalytic current increases steadily with the concentration of the added acid, Fig. 8. Compared to the potential (*ca.* 1.9 V) for proton reduction in the absence of complex **1**, the improvement in over-potential is not substantial. Since complex **1** cannot be protonated with this acid prior to reduction, the catalysis should be attributed to the species of the reduced complex **1**.

Catalytic responses of complex 2H^+ toward this weak acid are also investigated, Fig. 9. For the second reduction, the catalysis is rather similar to that observed for complex **1** (Fig. 8). Therefore, the second catalytic process is attributed to the *in situ* generated complex **1**. For the first reduction, a slight increase in current was observed but it rapidly levelled off. This minor increase may be due to kinetically controlled catalytic reduction of protons. It may also comprise contribution from the suppression of the dissociation of complex 2H^+ in the presence of the acid, Scheme 3, which effectively increased

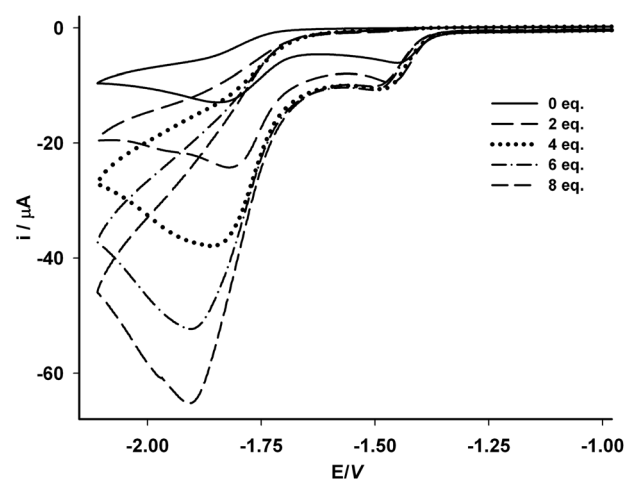


Fig. 9 Electrochemical responses of complex 2H^+ (3.4 mmol L^{-1}) upon addition of lutidinium under an Ar atmosphere in dichloromethane at the scanning rate of 0.1 V s^{-1} at 298 K.

the equilibrium concentration of this protonated complex 2H^+ . Whatever the origin of this increase is, the first reduction does not effectively catalyse proton reduction when this weak acid was employed.

When a strong acid is used, for example $\text{HBF}_4 \cdot \text{Et}_2\text{O}$, the electrochemistry of both complexes **1** and 2H^+ converges to that of complex 2H^+ in that the protonation of complex **1** forms effectively complex 2H^+ . As shown in Fig. 10 and 11, the protonated hexacarbonyl complex catalyses proton reduction under both Ar and CO atmospheres. The catalytic peak current against the acid concentration shows good linearity with coefficients over 0.99 in both cases, Fig. S14.† Contrary to CO-poisoning encountered by precious metal catalysts, the catalysis is enhanced rather than suppressed under a CO atmosphere. Furthermore, the catalysis under a CO atmosphere pro-

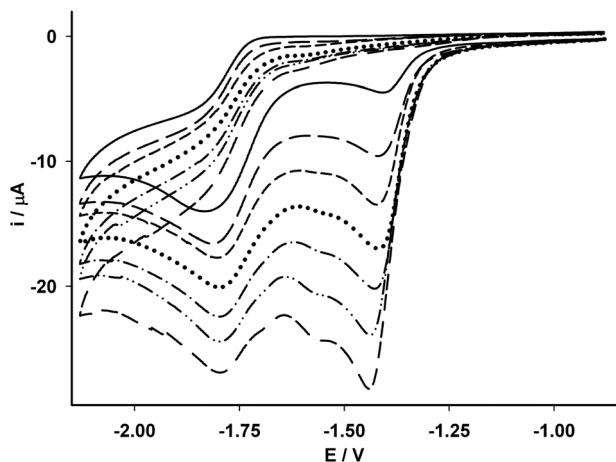


Fig. 10 Catalysing proton reduction by the associated species in the dichloromethane solution of complex 2H^+ (3.7 mmol L^{-1}) in the presence of the acid $\text{HBF}_4 \cdot \text{Et}_2\text{O}$ varying from 1 to 6 equivalents under an Ar atmosphere at the scanning rate of 0.1 V s^{-1} at 298 K.

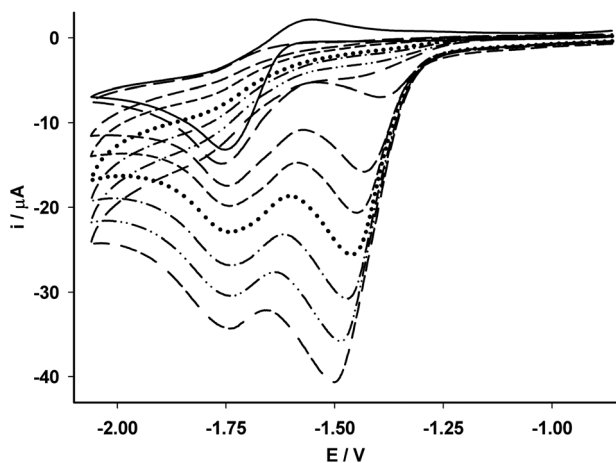


Fig. 11 Catalysing proton reduction by the associated species in the dichloromethane solution of complex 2H^+ (4.0 mmol L^{-1} , *in situ* generated by the addition of one equivalent of the acid) in the presence of the acid $\text{HBF}_4 \cdot \text{Et}_2\text{O}$ (from 1 to 6 equivalents) under a CO atmosphere at the scanning rate of 0.1 V s^{-1} at 298 K.

ceeded more cleanly as indicated by the cyclic voltammograms, Fig. 11. The CO-enhanced catalytic behaviour is probably due to the fact that the dissociation of complex 2H^+ is suppressed by CO, Scheme 3, on the one hand. On the other hand, the presence of CO may also suppress any processes involving CO-loss which may occur for iron-carbonyl complexes upon reduction. Most importantly, as shown in Scheme 3, under a CO atmosphere, the bound internal base pyridinyl group becomes pendant. The pendant pyridinyl group can be protonated and hence relay protons between the metal centre and the proton in bulk solution. It is noteworthy that the peak potential shifts for the second process. As contribution of the ir-drop increases with current intensity, the peak potential for reduction ought to shift negatively with the

increase of acid concentration. But this did not occur for the second process under either a CO or Ar atmosphere, Fig. 10 and 11. Instead, the peak potential steadily shifted positively. This is not completely surprising since in acidic medium, the catalytic species ought to be the species derived from the reduction of complex **1** and subsequent protonation rather than the directly reduced complex. These species catalyse proton reduction at more positive potentials.

3 Experimental section

All chemicals were used as purchased, unless otherwise stated. Freshly distilled solvents were used when necessary and manipulations under an inert atmosphere using Schlenk technique were employed in synthesis when appropriate. Electrochemistry was carried out under an argon atmosphere in dry solvent on Autolab Potentiostat 30. A conventional three-electrode system was employed in which a vitreous carbon disk ($\phi = 1 \text{ mm}$) was used as a working electrode, a vitreous carbon strip as a counter electrode and AgCl/Ag (Metrohm) as a reference electrode whose inner reference solution is composed of $0.05 \text{ mol L}^{-1} [\text{NBu}_4]\text{Cl}$ and $0.45 \text{ mol L}^{-1} [\text{NBu}_4]\text{BF}_4$. In dichloromethane, the electrolyte concentration is $0.5 \text{ mol L}^{-1} [\text{NBu}_4]\text{BF}_4$. All the potentials have been calibrated *versus* the Fc^+/Fc redox couple (0.55 V *versus* AgCl/Ag electrode in dichloromethane). Solution FTIR spectra were recorded on a Varian Scimitar 2000 using a solution cell with a spacer of 0.1 mm . UV/Vis measurements were performed on an Agilent 8453. NMR spectra were obtained on a Bruker Avance DRX 400 MHz. Micro analysis service was provided by Nanjing University (China). Procedures for organic synthesis are included in the ESI.†

3.1 $[\text{Fe}_2\{(\text{SCH}_2)_2\text{C}(\text{CH}_3)(2\text{-Py})\}(\text{CO})_5]$, **1**

To a solution of $\text{Fe}_3(\text{CO})_{12}$ (0.216 g , 0.4 mmol) in dry toluene (5 mL) was added a solution of 2-methyl-2-(pyridin-2-yl)propane-1,3-dithiol (0.079 g , 0.4 mmol) in dry toluene (10 mL) under N_2 . The reaction was heated at $110 \text{ }^\circ\text{C}$ for 4 hours under stirring. After removing the solvent, the reaction residues were purified using flash chromatography (eluting system: a mixture of ethyl acetate and *n*-hexane at a ratio of 1 : 4). A greenish brown band was collected. The removal of the solvents under vacuum yielded a black-green solid. The obtained product was re-dissolved in CH_3CN (10 mL) and insoluble materials were filtered off under N_2 . Both slow evaporation and storing at a low temperature ($-20 \text{ }^\circ\text{C}$) of the filtrate gave single crystals suitable for X-ray diffraction structural determination. FTIR (CH_3CN) ν_{CO} : 2048.6 , 1978.2 , 1914.1 cm^{-1} ; ^1H NMR (CDCl_3 , ppm): 1.49 (s, 3H), 1.88 (d, 2H, $J = 12.0 \text{ Hz}$), 2.04 (d, 2H, $J = 11.8 \text{ Hz}$), 7.15 (broad, 1H), 7.42 (broad, 1H), 7.70 (broad, 1H), 9.51 (broad, 1H). ^{13}C NMR (CDCl_3 , ppm): 31.4 , 31.7 , 48.1 , 77.3 , 122.6 , 123.6 , 137.9 , 159.2 , 166.6 , 208.6 , 210.9 . MS (ES): $(\text{M} + 1)/z = 450.8$, $(\text{M} - \text{CO} + 1)/z = 422.3$. Microanalysis (%) for $\text{C}_{14}\text{H}_{11}\text{NO}_5\text{S}_2\text{Fe}_2$ (449.07), calculated (found): C, 37.44 (37.40); H, 2.47 (2.50); N, 3.12 (3.15).

3.2 $[\text{Fe}_2\{(\text{SCH}_2)_2\text{C}(\text{CH}_3)(2\text{-HPy})\}(\text{CO})_6]^+, 2\text{H}^+$

Complex **1** (13.7 mg, 3.05 mmol) was dissolved in dry toluene (10 mL). Then the solution was saturated with CO and 1 eq. $\text{HBF}_4 \cdot \text{Et}_2\text{O}$ (4.28 μl) was added under CO on stirring at room temperature and a reddish precipitate appeared instantly to give nearly quantitative conversion of **1** to the protonated complex 2H^+ . The solid was collected, washed with dry toluene and dried under vacuum. A solution of the red precipitate in dichloromethane at a low temperature (-20°C) produced red single crystals suitable for X-ray diffraction analysis. FTIR (DCM with $\text{HBF}_4 \cdot \text{Et}_2\text{O}$) ν_{CO} : 2079.5, 2038.9, 2011.5, 2001.8 cm^{-1} . Due to its instability, the complex was not further characterised except for electrochemistry.

4 Conclusion remarks

The synthesis, characterisation, inter-conversion, and electrochemical and electrocatalytic investigations of two diiron complexes **1** and 2H^+ which possess an integrated pyridine/pyridinium group were reported. The inter-conversion of the two complexes proceeds *via* the intermediate **2**, the deprotonated form of complex 2H^+ . Upon protonation, the inter-conversion equilibrium strongly shifts to the formation of complex 2H^+ even under an Ar/ N_2 atmosphere, in which the need for the CO molecule is met by “cannibalisation”. In complex **1**, the bond Fe–N (pyridine) is hemi-labile and subject to protonation. Although no hexacarbonyl species (**2**) can be detected in the solution of complex **1** under an Ar/ N_2 atmosphere, the content of complex **2** could be over 5% in the presence of CO.³³ Under a CO atmosphere, complex **1** shows unusual electrochemistry which is attributed to the existence of the equilibrium between complexes **1** and **2**. Complex 2H^+ exhibits two reductions rather than one and the first one occurs at a more positive potential due to its positive charge. Furthermore, the second reduction is much stronger than the first one. This reduction is assigned to the reduction processes of complex **1** generated *in situ*. Complex 2H^+ shows catalysis towards proton reduction in the presence of $\text{HBF}_4 \cdot \text{Et}_2\text{O}$ at its first reduction, which is enhanced in the presence of CO due to mainly the presence of CO which helps free the bound pyridinyl group. The freed base group acts as a proton relay to enhance the catalysis. Thus, our results and reports in the literature^{24–26} suggest strongly that an internal base has a role to play in improving the catalysis of proton reduction.

Acknowledgements

We thank the Natural Science Foundation of China (Grant No. 20871064, 21571083, 21365015), the Educational Commission of Jiangxi Province (Grant No. GJJ13109) and the Government of Zhejiang Province (Qianjiang professorship for XL) for supporting this work. We are grateful for the suggestion from Professor Pickett (University of East Anglia, UK).

References

- J. W. Peters, W. N. Lanzilotta, B. J. Lemon and L. C. Seefeldt, *Science*, 1998, **282**, 1853–1858.
- Y. Nicolet, C. Piras, P. Legrand, C. E. Hatchikian and J. C. Fontecilla-Camps, *Structure*, 1999, **7**, 13–23.
- E. M. Shepard, F. Mus, J. N. Betz, A. S. Byer, B. R. Duffus, J. W. Peters and J. B. Broderick, *Biochemistry*, 2014, **53**, 4090–4104.
- P. Dinis, D. L. M. Suess, S. J. Fox, J. E. Harmer, R. C. Driesener, L. De La Paz, J. R. Swartz, J. W. Essex, R. D. Britt and P. L. Roach, *Proc. Natl. Acad. Sci. U. S. A.*, 2015, **112**, 1362–1367.
- I. P. Georgakaki, L. M. Thomson, E. J. Lyon, M. B. Hall and M. Y. Darensbourg, *Coord. Chem. Rev.*, 2003, **238**, 255–266.
- L. C. Sun, B. Akermark and S. Ott, *Coord. Chem. Rev.*, 2005, **249**, 1653–1663.
- X. M. Liu, S. K. Ibrahim, C. Tard and C. J. Pickett, *Coord. Chem. Rev.*, 2005, **249**, 1641–1652.
- J. F. Capon, F. Gloaguen, P. Schollhammer and J. Talarmin, *Coord. Chem. Rev.*, 2005, **249**, 1664–1676.
- C. Tard and C. J. Pickett, *Chem. Rev.*, 2009, **109**, 2245–2274.
- W. Lubitz, H. Ogata, O. Rüdiger and E. Reijerse, *Chem. Rev.*, 2014, **114**, 4081–4148.
- Y. Li and T. B. Rauchfuss, *Chem. Rev.*, 2016, **116**, 7043–7077.
- D. Schilter, J. M. Camara, M. T. Huynh, S. Hammes-Schiffer and T. B. Rauchfuss, *Chem. Rev.*, 2016, **116**, 8693–8749.
- M. Razavet, S. C. Davies, D. L. Hughes, J. E. Barclay, D. J. Evans, S. A. Fairhurst, X. M. Liu and C. J. Pickett, *Dalton Trans.*, 2003, 586–595.
- X. F. Wang, Z. M. Li, X. R. Zeng, Q. Y. Luo, D. J. Evans, C. J. Pickett and X. M. Liu, *Chem. Commun.*, 2008, 3555–3557.
- C. Tard, X. M. Liu, S. K. Ibrahim, M. Bruschi, L. De Gioia, S. C. Davies, X. Yang, L. S. Wang, G. Sawers and C. J. Pickett, *Nature*, 2005, **433**, 610–613.
- J.-F. Capon, F. Gloaguen, F. Y. Pétilion, P. Schollhammer and J. Talarmin, *Coord. Chem. Rev.*, 2009, **253**, 1476–1494.
- F. Gloaguen and T. B. Rauchfuss, *Chem. Soc. Rev.*, 2009, **38**, 100–108.
- G. A. N. Felton, C. A. Mebi, B. J. Petro, A. K. Vannucci, D. H. Evans, R. S. Glass and D. L. Lichtenberger, *J. Organomet. Chem.*, 2009, **694**, 2681–2699.
- G. Qian, W. Zhong, Z. Wei, H. Wang, Z. Xiao, L. Long and X. Liu, *New J. Chem.*, 2015, **39**, 9752–9760.
- G. Qian, H. Wang, W. Zhong and X. Liu, *Electrochim. Acta*, 2015, **163**, 190–195.
- X. Zeng, Z. Li, Z. Xiao, Y. Wang and X. Liu, *Electrochem. Commun.*, 2010, **12**, 342–345.
- G. Berggren, A. Adamska, C. Lambert, T. R. Simmons, J. Esselborn, M. Atta, S. Gambarelli, J. M. Mouesca, E. Reijerse, W. Lubitz, T. Happe, V. Artero and M. Fontecave, *Nature*, 2013, **499**, 66–69.

- 23 M. R. DuBois and D. L. DuBois, *Chem. Soc. Rev.*, 2009, **38**, 62–72.
- 24 R. M. Henry, R. K. Shoemaker, D. L. DuBois and M. R. DuBois, *J. Am. Chem. Soc.*, 2006, **128**, 3002–3010.
- 25 N. Wang, M. Wang, T. T. Zhang, P. Li, J. H. Liu and L. C. Sun, *Chem. Commun.*, 2008, 5800–5802.
- 26 S. Ezzaher, J. F. Capon, F. Gloaguen, F. Y. Petillon, P. Schollhammer, J. Talarmin and N. Kervarec, *Inorg. Chem.*, 2009, **48**, 2–4.
- 27 Y. Wang, M. Wang, L. C. Sun and M. S. G. Ahlquist, *Chem. Commun.*, 2012, **48**, 4450–4452.
- 28 N. Wang, M. Wang, L. Chen and L. C. Sun, *Dalton Trans.*, 2013, **42**, 12059–12071.
- 29 J. D. Lawrence, H. X. Li and T. B. Rauchfuss, *Chem. Commun.*, 2001, 1482–1483.
- 30 S. Ott, M. Kritikos, B. Akermark, L. C. Sun and R. Lomoth, *Angew. Chem., Int. Ed.*, 2004, **43**, 1006–1009.
- 31 P. Y. Orain, J. F. Capon, N. Kervarec, F. Gloaguen, F. Petillon, R. Pichon, P. Schollhammer and J. Talarmin, *Dalton Trans.*, 2007, 3754–3756.
- 32 L. L. Duan, M. Wang, P. Li, Y. Na, N. Wang and L. C. Sun, *Dalton Trans.*, 2007, 1277–1283.
- 33 F. F. Xu, C. Tard, X. F. Wang, S. K. Ibrahim, D. L. Hughes, W. Zhong, X. R. Zeng, Q. Y. Luo, X. M. Liu and C. J. Pickett, *Chem. Commun.*, 2008, 606–608.
- 34 S. Friedrich, M. Schubart, L. H. Gade, I. J. Scowen, A. J. Edwards and M. McPartlin, *Chem. Ber./Recl.*, 1997, **130**, 1751–1759.
- 35 M. Razavet, S. C. Davies, D. L. Hughes and C. J. Pickett, *Chem. Commun.*, 2001, 847–848.
- 36 Z. Y. Xiao, F. F. Xu, L. Long, Y. Q. Liu, G. Zampella, L. De Gioia, X. R. Zeng, Q. Y. Luo and X. M. Liu, *J. Organomet. Chem.*, 2010, **695**, 721–729.
- 37 R. Linnell, *J. Org. Chem.*, 1960, **25**, 290–290.
- 38 P. Bonvicin, A. Levi, V. Lucchini and G. Scorrano, *J. Chem. Soc., Perkin Trans. 2*, 1972, 2267–2269.
- 39 S. J. George, Z. Cui, M. Razavet and C. J. Pickett, *Chem. – Eur. J.*, 2002, **8**, 4037–4046.
- 40 M. Razavet, A. Le Cloirec, S. C. Davies, D. L. Hughes and C. J. Pickett, *J. Chem. Soc., Dalton Trans.*, 2001, 3551–3552.
- 41 D. Seyferth, G. B. Womack, M. K. Gallagher, M. Cowie, B. W. Hames, J. P. Fackler and A. M. Mazany, *Organometallics*, 1987, **6**, 283–294.
- 42 L. C. Song, Z. Y. Yang, Y. J. Hua, H. T. Wang, Y. Liu and Q. M. Hu, *Organometallics*, 2007, **26**, 2106–2110.
- 43 L. Luan, M. Brookhart and J. L. Templeton, *Organometallics*, 1992, **11**, 1433–1435.
- 44 L. D. Field, W. J. Shaw and G. K. B. Clentsmith, *J. Organomet. Chem.*, 2007, **692**, 3042–3047.
- 45 R. G. Pearson and P. C. Ford, *Comments Inorg. Chem.*, 1982, **1**, 279–291.
- 46 S. J. Borg, T. Behrsing, S. P. Best, M. Razavet, X. M. Liu and C. J. Pickett, *J. Am. Chem. Soc.*, 2004, **126**, 16988–16999.
- 47 R. Mejia-Rodriguez, D. S. Chong, J. H. Reibenspies, M. P. Soriaga and M. Y. Darensbourg, *J. Am. Chem. Soc.*, 2004, **126**, 12004–12014.
- 48 Z. Wang, W. F. Jiang, J. H. Liu, W. I. Jiang, Y. Wang, B. Akermark and L. C. Sun, *J. Organomet. Chem.*, 2008, **693**, 2828–2834.